

Neutron diffraction studies on $(\text{Ho}_{1-x}\text{Er}_x)_2\text{Fe}_{15}\text{Ga}_2\text{C}_y$ compounds

M. Venkatesan, U. V. Varadaraju, K. V. S. Rama Rao, S. K. Malik, H. Luo, and W. B. Yelon

Citation: *Journal of Applied Physics* **86**, 3290 (1999); doi: 10.1063/1.371204

View online: <http://dx.doi.org/10.1063/1.371204>

View Table of Contents: <http://scitation.aip.org/content/aip/journal/jap/86/6?ver=pdfcov>

Published by the [AIP Publishing](#)

Articles you may be interested in

[Structural, magnetic and magnetostrictive properties of Co-doped \$\text{Tb}_{1-x}\text{Ho}_x\text{Fe}_2\$ \(\$0 \leq x \leq 1.0\$ \) alloys](#)

J. Appl. Phys. **110**, 073915 (2011); 10.1063/1.3647757

[Magnetic phase transition and Mössbauer spectroscopy of \$\text{ErNi}_2\text{Mn}_x\$ compounds](#)

J. Appl. Phys. **109**, 07E304 (2011); 10.1063/1.3535544

[Structure and magnetic properties of \$\(\text{Nd}_{1-x}\text{Ho}_x\)_3\text{Fe}_{23-y}\text{Co}_6\text{V}_y\$ compounds](#)

J. Appl. Phys. **93**, 6927 (2003); 10.1063/1.1544492

[A neutron diffraction structural study of \$\text{R}_2\text{Fe}_{17-x}\text{Al}_x\(\text{C}\)\$ \(\$\text{R}=\text{Tb}, \text{Ho}\$ \) alloys](#)

J. Appl. Phys. **83**, 6914 (1998); 10.1063/1.367567

[Effect of Ga substitution on the structure and magnetic properties of \$\text{Ho}_2\text{Fe}_{17-x}\text{Ga}_x\$ \(\$x=0-8\$ \) compounds](#)

J. Appl. Phys. **83**, 3250 (1998); 10.1063/1.367092



Neutron diffraction studies on $(\text{Ho}_{1-x}\text{Er}_x)_2\text{Fe}_{15}\text{Ga}_2\text{C}_y$ compounds

M. Venkatesan

Materials Science Research Centre, Department of Physics, Indian Institute of Technology, Madras 600 036, India

U. V. Varadaraju^{a)}

Materials Science Research Centre, Indian Institute of Technology, Madras 600 036, India

K. V. S. Rama Rao

Department of Physics, Indian Institute of Technology, Madras 600 036, India

S. K. Malik

Tata Institute of Fundamental Research, Mumbai 400 005, India

H. Luo and W. B. Yelon

University of Missouri Research Reactor Facility, Columbia, Missouri 65211

(Received 25 January 1999; accepted for publication 10 June 1999)

Powder neutron diffraction studies were carried out on $(\text{Ho}_{1-x}\text{Er}_x)_2\text{Fe}_{15}\text{Ga}_2\text{C}_y$ ($x=0, 0.5, 1$; $y=0, 2$) with a view to study the effect of substitution of Ga for Fe and the insertion of carbon at the interstitial sites on the structural and magnetic properties. All Ga substituted compounds ($y=0$) possess hexagonal $\text{Th}_2\text{Ni}_{17}$ type structure (space group: $P6_3/mmc$). However, the carbides adopt rhombohedral $\text{Th}_2\text{Zn}_{17}$ type structure (Space group: $R\bar{3}m$). The unit cell volume increases with Ga substitution as well as with interstitial modification by carbon. An increase in the Curie temperature of about 260 K is observed for the compound $\text{HoErFe}_{15}\text{Ga}_2\text{C}_2$ vis-a-vis HoErFe_{17} . The increase is attributed to the preferential occupancy of Ga atoms in $18f(12j)$ and $18h(12k)$ sites and the presence of interstitial carbon. The magnetization increases with carbon addition. X-ray diffraction studies on magnetically aligned samples and neutron diffraction studies show that the easy magnetization direction lies in the basal plane at room temperature. © 1999 American Institute of Physics. [S0021-8979(99)05718-7]

I. INTRODUCTION

The binary rare earth (*R*)-iron intermetallic compounds based on the $R_2\text{Fe}_{17}$ structure evoke much interest owing to their ability to accommodate lighter elements into octahedral interstitial sites.¹ The low value of Curie temperature of these compounds is usually attributed to the short Fe-Fe distance at the dumb-bell site as well as due to the effect of negative exchange interaction among the iron atoms.^{2,3} These compounds crystallize in the hexagonal $\text{Th}_2\text{Ni}_{17}$ type structure (space group: $P6_3/mmc$) for heavy rare earths or rhombohedral $\text{Th}_2\text{Zn}_{17}$ type structure (space group: $R\bar{3}m$) for lighter rare earths. The hexagonal $\text{Th}_2\text{Ni}_{17}$ type structure has two crystallographically inequivalent sites ($2b$ and $2d$) for the rare earths and four inequivalent sites ($4f$, $12j$, $12k$, and $6g$) for iron whereas the rhombohedral $\text{Th}_2\text{Zn}_{17}$ type structure has one rare earth site ($6c$) and four iron sites ($6c$, $18f$, $18h$, and $9d$). The dramatic increase in Curie temperature and uniaxial anisotropy in these compounds with insertion of nitrogen or carbon has led to a renewed interest in these compounds.^{1,4,5} It is believed that the lengthened Fe-Fe bonds with enhanced ferromagnetic exchange play an important role in the increase of Curie temperature. The role of interstitial atoms is to eliminate the antiferromagnetic cou-

pling between Fe-Fe pairs in the structure by lattice expansion. This can also be effected by replacing some of the iron by an element with a larger metallic radius. We have previously reported that the nonmagnetic substitution in $R_2\text{Fe}_{17}$ to produce $R_2\text{Fe}_{17-x}\text{M}_x$ ($M=\text{Al, Ga}$) solid solutions leads to an enhanced Curie temperature accompanied by unit cell volume expansion.^{6,7} However, for Si substituted $R_2\text{Fe}_{17}$ compounds, the Curie temperature increases with decreasing unit cell volume.¹⁵ In addition, the rare earth sublattice anisotropy could be increased by a proper choice of rare earths, provided there exists a preferential occupancy of the sites, rendering the magnetization axial at both sites ($2b$ and $2d$ in the hexagonal unit cell).⁸ It is well known that the product $\alpha_J A_{20}$ (α_J is the Steven's coefficient and A_{20} is the second order crystal field parameter) should be negative to have large rare earth sublattice anisotropy. In $R_2\text{Fe}_{17}$ compounds, the sign of A_{20} is found to be negative.⁹ Although the transition metal sublattice magnetization is considerably reduced by the nonmagnetic element by dilution effects, the possibility of attaining materials with high Curie temperature and uniaxial anisotropy is still worth exploring. In continuation of our earlier reports concerning the effect of Ga on Curie temperature and magnetic anisotropy in HoErFe_{17} compounds⁷ and their carbides,¹⁰ we report here a neutron diffraction study on $(\text{Ho}_{1-x}\text{Er}_x)_2\text{Fe}_{15}\text{Ga}_2\text{C}_y$ ($x=0, 0.5, 1$; $y=0, 2$) phases in which Ho has negative α_J and Er has posi-

^{a)}Fax No: 044-235 0509. Electronic mail: raju@msrc.iitm.ernet.in

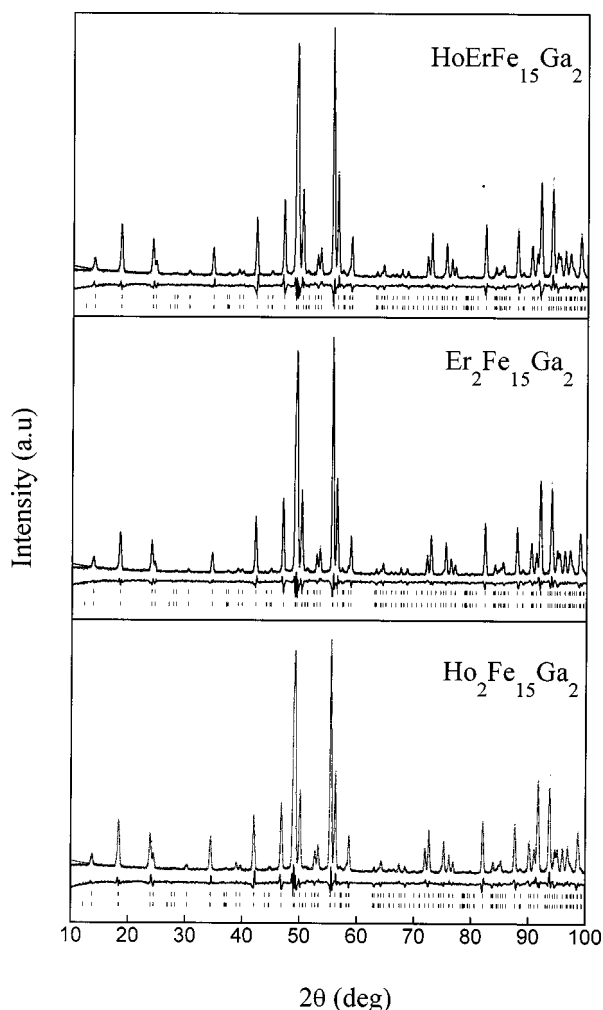


FIG. 1. Neutron diffraction patterns of $(\text{Ho}_{1-x}\text{Er}_x)_2\text{Fe}_{15}\text{Ga}_2$ ($x=0, 0.5,$ and 1) at room temperature. The points and the curve refer to the recorded pattern and the calculated fit, respectively. A difference pattern is plotted in the lower part of the figure. The first and second sets of bars refer to the nuclear and magnetic diffraction peaks.

tive α_j and the detailed analysis of the effects produced by carbonation, in particular, on the crystallographic structure and magnetic properties.

II. EXPERIMENT

The compounds with compositions $(\text{Ho}_{1-x}\text{Er}_x)_2\text{Fe}_{15}\text{Ga}_2\text{C}_y$ ($x=0, 1; y=0, 2$) were synthesized by arc melting the stoichiometric amounts of high pure starting elements (Ho, Er, Ga, C: 99.9%; Fe: 99.99%) in high pure argon atmosphere. Due to the high melting point of carbon, Fe and C were melted together first to form Fe_3C (cementite) which has a lower melting temperature. Fe_3C is then mixed with remaining constituent elements and melted to form an ingot. The ingots were remelted several times to ensure homogeneity. The samples were then wrapped in tantalum foils and annealed at 1100°C for three days. In order to avoid the formation of $\text{R}_2\text{Fe}_{14}\text{C}$ phase during cooling, the ingots were quenched from the annealing temperature in cold water. Neutron diffraction data were collected at the University of Missouri Research Reactor using the high resolution linear position-sensitive detector diffractometer. The neutron

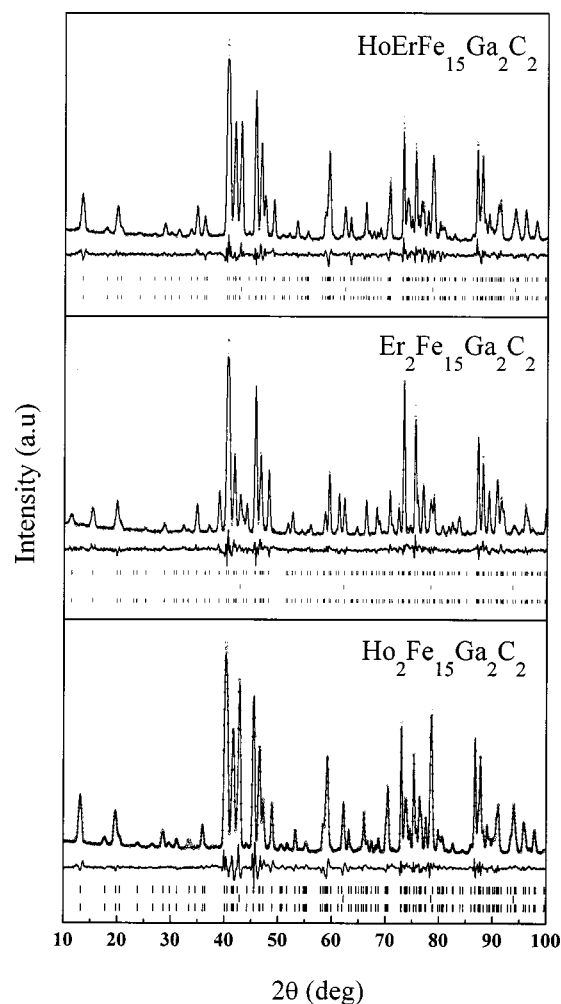


FIG. 2. Neutron diffraction patterns of $(\text{Ho}_{1-x}\text{Er}_x)_2\text{Fe}_{15}\text{Ga}_2\text{C}_2$ ($x=0, 0.5,$ and 1) at room temperature. The points and the curve refer to the recorded pattern and the calculated fit, respectively. A difference pattern is plotted in the lower part of the figure. The first and third sets of bars refer to the nuclear and magnetic diffraction peaks. The second set refer to α -Fe as impurity.

wavelength was 1.4783 \AA . Approximately $2g$ of finely powdered samples were contained in thin walled vanadium holders. The data for each sample were collected at room temperature (which is below Curie temperature for all samples) with 2θ values 5° to 105° in 0.05° steps. Refinements of the neutron diffraction data were carried out by the Rietveld method with the FULLPROF computer code which permits multiple phase refinement as well as magnetic structure refinement.^{11,12} The Curie temperatures were determined from the temperature dependence of the magnetization measured with a vibrating sample magnetometer in a magnetic field of 500 Oe . The aligned samples for determining easy magnetization direction (EMD) were prepared by mixing the powder with epoxy resin and subsequently aligning in a magnetic field of 20 kOe .

III. RESULTS AND DISCUSSION

The observed diffraction lines are a result of both nuclear and magnetic scattering, because the data were collected below Curie temperature. Before analyzing the neu-

TABLE I. The lattice parameters, atomic coordinates, site occupancies, and magnetic moments in $(\text{Ho}_{1-x}\text{Er}_x)_2\text{Fe}_{15}\text{Ga}_2\text{C}_y$ ($x=0, 0.5, 1; y=0, 2$) compounds.

Hexagonal system	$\text{Ho}_2\text{Fe}_{15}\text{Ga}_2$	$\text{Er}_2\text{Fe}_{15}\text{Ga}_2$	$\text{HoErFe}_{15}\text{Ga}_2$	Rhombohedral system	$\text{Ho}_2\text{Fe}_{15}\text{Ga}_2\text{C}_2$	$\text{Er}_2\text{Fe}_{15}\text{Ga}_2\text{C}_2$	$\text{HoErFe}_{15}\text{Ga}_2\text{C}_2$
a , (Å)	8.5263(2)	8.5139(2)	8.5218(2)	a , Å	8.6595(3)	8.6353(2)	8.6572(3)
c , (Å)	8.3390(2)	8.3313(2)	8.3326(2)	c , Å	12.5329(5)	12.5414(3)	12.5396(5)
v , Å ³	525	523	524	v , Å ³	813.89	809.9	813.88
Ho/Er, $2b$, z	0.25	0.25	0.25	Ho/Er, $6c$, z	0.3405(4)	0.3392(1)	0.3376(4)
Ho/Er, $2d$, x	0.3333	0.3333	0.3333	Fe/Ga, $6c$, z	0.0963(2)	0.0964(2)	0.0964(2)
Ho/Er, $2d$, y	0.6666	0.6666	0.6666				
Ho/Er, $2d$, z	0.75	0.75	0.75				
Fe/Ga, $4f$, x	0.3333	0.3333	0.3333	Fe/Ga, $18f$, x	0.2836(2)	0.2838(1)	0.2849(2)
y	0.6666	0.6666	0.6666				
z	0.1076(3)	0.1068(2)	0.1066(4)				
Fe/Ga, $12j$, x	0.3305(3)	0.3301(1)	0.3299(3)	Fe/Ga, $18h$, x	0.1691(1)	0.1690(1)	0.1690(1)
y	-0.0415(2)	-0.0411(3)	-0.0417(2)	z	0.4872(1)	0.4874(2)	0.4886(1)
z	0.25	0.25	0.25				
Fe/Ga, $12k$, x	0.1666(4)	0.1670(2)	0.1669(4)	Fe/Ga, $9d$, x	0.5	0.5	0.5
y	0.3333(4)	0.3342(3)	0.3341(4)	z	0.5	0.5	0.5
z	0.9834(2)	0.9826(2)	0.9829(2)				
Fe/Ga, $6g$, x	0.5	0.5	0.5				
%Ga $4f$	%Ga $6c$
%Ga $12j$	13.6	14.8	14.2	%Ga $18f$	14.5	15.3	14.2
%Ga $12k$	19.4	18.2	18.7	%Ga $18h$	18.4	17.2	17.8
%Ga $6g$	%Ga $9d$
μ , Ho/Er, $2b$, μ_B	-4.6(1)	-2.9(1)	-3.6(1)	μ , Ho/Er, $6c$, μ_B	-3.4(1)	-2.3(1)	-2.7(1)
μ , Ho/Er, $2d$, μ_B	-4.6(1)	-2.9(1)	-3.6(1)	μ , Fe, $6c$, μ_B	-3.0(1)	-2.9(1)	-2.9(1)
μ , Fe, $4f$, μ_B	2.1(2)	2.1(1)	2.4(1)	μ , Fe, $18f$, μ_B	1.7(2)	1.8(2)	1.8(2)
μ , Fe, $12j$, μ_B	2.0(2)	2.4(1)	2.4(2)	μ , Fe, $18h$, μ_B	1.3(2)	1.3(2)	1.3(1)
μ , Fe, $12k$, μ_B	1.6(1)	2.0(1)	2.0(1)	μ , Fe, $9d$, μ_B	2.1(2)	2.3(1)	2.1(1)
μ , Fe, $6g$, μ_B	1.0(1)	1.2(2)	1.2(1)	μ , cell, μ_B	64.8	73.8	69.3
μ , cell, μ_B	31.0	47.1	44.4	μ , formula, μ_B	21.6	24.6	23.1
μ , formula, μ_B	15.5	23.5	22.1				
R_p factor	5.60	5.88	5.05	R_p factor	5.28	4.91	4.97
R_{wp} factor	7.38	7.55	7.81	R_{wp} factor	7.14	6.38	6.58
R_m factor	7.70	7.28	6.07	R_m factor	7.38	6.92	5.42

neutron diffraction data, it was confirmed that all the Ga substituted compounds possess hexagonal structure whereas their carbides crystallize in rhombohedral symmetry. Therefore, the neutron diffraction patterns were analyzed on the basis of a hexagonal cell (space group: $P6_3/mmc$) for Ga substituted compounds and rhombohedral cell (space group $R\bar{3}m$) for their corresponding carbides. The calculated patterns along with observed ones are shown in Figs. 1 and 2. In the case of carbides, there is an increase in the α -Fe contribution. The fraction of α -Fe obtained from the refinement increases from 1.8% for compounds without carbon to about 9% for the corresponding carbides. The results of the refinement viz., lattice parameters, atomic coordinates, the occupancy of Ga atoms at various sites and magnetic moments are shown in Table I. The value of thermal parameters obtained for various elements in the different compounds are in the range 1.0–1.3 for Ho/Er, 0.9–1.2 for Ho, 0.6–0.8 for C. Insertion of carbon at the interstitial sites results in structural transformation from hexagonal to rhombohedral symmetry. This is in contrast to the $R_2\text{Fe}_{17}\text{N}_y$ compounds, where the presence of interstitial nitrogen does not change the structure. The

lattice parameters “ a ” and “ c ” and the unit cell volume “ V ” increase with substitution of Ga and insertion of carbon suggesting the expansion of Fe–Fe bonds. The unit cell volume expansion is 2.9% and 6.4% for $\text{HoErFe}_{15}\text{Ga}_2$ and $\text{HoErFe}_{15}\text{Ga}_2\text{C}_2$, respectively, compared to HoErFe_{17} . The unit cell parameters obtained from neutron diffraction measurements agree well with those calculated from x-ray diffraction data for all compounds.

The parameters of the crystallographic structure of the $\text{Th}_2\text{Ni}_{17}$ and $\text{Th}_2\text{Zn}_{17}$ type rare earth iron compounds were used as the starting model for refining Ga substituted compounds and their carbides, respectively. In the present study, it is assumed that the iron and gallium atoms occupy $18h$, $18f$, $9d$, and $6c$ sites in the case of carbides (rhombohedral structure) whereas the iron and gallium atoms occupy $12k$, $12j$, $6g$, and $4f$ sites in the case of Ga substituted compounds (hexagonal structure). In addition, x-ray diffraction studies on $R_2\text{Mn}_{17}\text{C}_{3-\delta}$ ($\delta \sim 2$) and neutron diffraction studies on $\text{Nd}_2\text{Fe}_{17}\text{C}_y$ compounds^{13–15} showed octahedral site occupancy for carbon ($9e$ in rhombohedral structure).

TABLE II. Curie temperature and room temperature magnetization (1.2 T) of $(\text{Ho}_{1-x}\text{Er}_x)_2\text{Fe}_{15}\text{Ga}_2\text{C}_y$ compounds.

Compound	T_C (K)	M (emu/g)
$\text{Ho}_2\text{Fe}_{17}^a$	327	65
$\text{Ho}_2\text{Fe}_{15}\text{Ga}_2$	498	67
$\text{Ho}_2\text{Fe}_{15}\text{Ga}_2\text{C}_2$	625	81
$\text{Er}_2\text{Fe}_{17}^a$	297	61
$\text{Er}_2\text{Fe}_{15}\text{Ga}_2$	477	72
$\text{Er}_2\text{Fe}_{15}\text{Ga}_2\text{C}_2$	607	89
HoErFe_{17}^b	328	64
$\text{HoErFe}_{15}\text{Ga}_2$	486	70
$\text{HoErFe}_{15}\text{Ga}_2\text{C}_2$	612	86

^aReference 9.

^bReference 7.

The Curie temperature of $(\text{Ho}_{1-x}\text{Er}_x)_2\text{Fe}_{15}\text{Ga}_2\text{C}_y$ are presented in Table II. The Curie temperature increases with both nonmagnetic Ga substitution and interstitial carbon addition. An increase in Curie temperature of 284 K is observed in the compound $\text{HoErFe}_{15}\text{Ga}_2\text{C}_2$ when compared to HoErFe_{17} .⁷ The increase in the Curie temperature, when iron is substituted by Ga can be attributed to the enhanced ferromagnetic exchange in the compound due to lattice expansion.

The nonmagnetic Ga atoms prefer 12*j* and 12*k* sites in the hexagonal structure whereas they prefer 18*h* sites preferentially and also 18*f* sites in rhombohedral structure as shown in Table I. The 9*d* crystallographic site (in rhombohedral $\text{Th}_2\text{Zn}_{17}$ type structure) which has the smallest Wigner–Seitz cell volume is avoided completely by Ga atoms. Since 9*d* is unoccupied by Ga atoms, there is a greater probability that its nearest neighbors (four 18*f* and four 18*h* iron atoms) have larger affinity to accept Ga. This accounts for high Ga occupancy at 18*f* and 18*h* sites. It has been shown in earlier studies that in $\text{Y}_2\text{Fe}_{17-x}\text{Si}_x$,¹⁶ nonmagnetic atom Si substitutes preferentially at 4*f*(6*c*) iron site in hexagonal (rhombohedral) structure whereas in $\text{Nd}_2\text{Fe}_{17-x}\text{Si}_x$,¹⁷ Si atoms prefer 18*h* site and avoid 6*c* sites. The increase in Curie temperature despite the unit cell volume contraction in Si substituted $R_2\text{Fe}_{17}$ compounds is mainly attributed to such preferential occupancy of Si atoms at antiferromagnetically coupled Fe sites.

In the Fe rich rare earth–iron intermetallic compounds, the Curie temperature is mainly determined by the Fe–Fe, R–Fe, and R–R interactions. In general, the Fe–Fe interac-

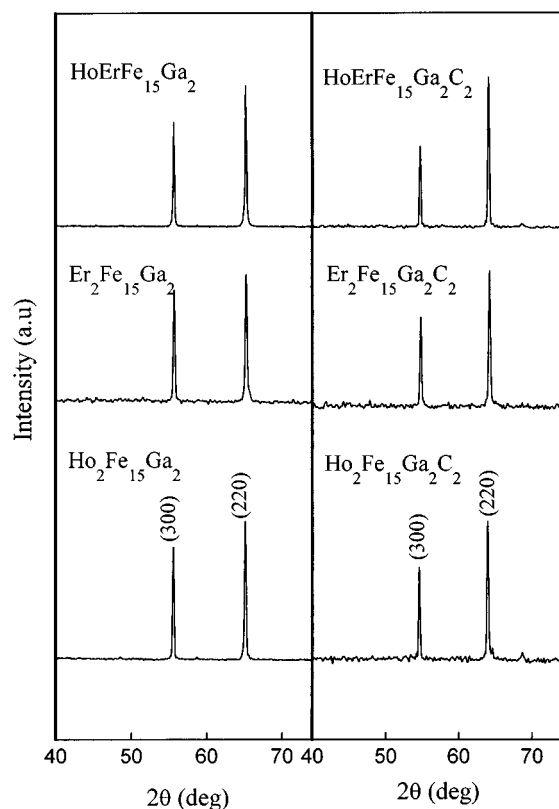


FIG. 3. X-ray diffractograms of magnetically aligned $(\text{Ho}_{1-x}\text{Er}_x)_2\text{Fe}_{15}\text{Ga}_2\text{C}_y$ ($x=0, 0.5, 1$, and $y=0, 2$) at room temperature.

tions are dominant and these are strong enough to dominate Curie temperature of the Fe-rich intermetallic compounds whereas, the R–R interactions are negligible. It is well known that $R_2\text{Fe}_{17}$ compounds possess both positive and negative interactions ($d < 2.45 \text{ \AA}$).¹⁸ The 6*c*–6*c* bond length (dumb-bell site) in rhombohedral $\text{Th}_2\text{Zn}_{17}$ type structure (4*f*–4*f* in hexagonal $\text{Th}_2\text{Ni}_{17}$ type) is the shortest of all bonds, which leads to low Curie temperature in $R_2\text{Fe}_{17}$ compounds. This implies that the magnitude and sign of the exchange interaction are mainly determined by the distances of the Fe–Fe pairs.

In the compounds with hexagonal structure, the Fe(4*f*)–Fe(4*f*) interactions are strongly negative whereas the Fe(6*g*)–Fe(12*j*), Fe(6*g*)–Fe(12*k*), and

TABLE III. Bond distance between Fe atoms at various Fe sites in $(\text{Ho}_{1-x}\text{Er}_x)_2\text{Fe}_{15}\text{Ga}_2\text{C}_y$ ($x=0, 0.5, 1$; $y=0, 2$) compounds.

Bond (hexagonal)	$\text{Ho}_2\text{Fe}_{15}\text{Ga}_2$ (Å)	$\text{Er}_2\text{Fe}_{15}\text{Ga}_2$ (Å)	$\text{HoErFe}_{15}\text{Ga}_2$ (Å)	Bond (rhombohedral)	$\text{Ho}_2\text{Fe}_{15}\text{Ga}_2\text{C}_2$ (Å)	$\text{Er}_2\text{Fe}_{15}\text{Ga}_2\text{C}_2$ (Å)	$\text{HoErFe}_{15}\text{Ga}_2\text{C}_2$ (Å)
Fe(4 <i>f</i>)–Fe(4 <i>f</i>)	2.3750(4)	2.3861(4)	2.3888(4)	Fe(6 <i>c</i>)–Fe(6 <i>c</i>)	2.4151(5)	2.4162(4)	2.4179(4)
Fe(4 <i>f</i>)–Fe(6 <i>g</i>)	2.6198(1)	2.6139(1)	2.6157(1)	Fe(6 <i>c</i>)–Fe(4 <i>f</i>)	2.7370(1)	2.6813(1)	2.7474(1)
Fe(4 <i>f</i>)–Fe(12 <i>j</i>)	2.7678(2)	2.7715(2)	2.7697(2)	Fe(6 <i>c</i>)–Fe(18 <i>h</i>)	2.6731(2)	2.6712(3)	2.6682(2)
Fe(4 <i>f</i>)–Fe(12 <i>k</i>)	2.6543(3)	2.6608(1)	2.6618(3)	Fe(6 <i>c</i>)–Fe(9 <i>d</i>)	2.6506(1)	2.6502(3)	2.6498(1)
Fe(12 <i>j</i>)–Fe(12 <i>j</i>)	2.5010(3)	2.5014(3)	2.4988(3)	Fe(18 <i>f</i>)–Fe(18 <i>f</i>)	2.4563(3)	2.4613(4)	2.4671(2)
Fe(12 <i>j</i>)–Fe(12 <i>k</i>)	2.5911(2)	2.5873(2)	2.5893(2)	Fe(18 <i>f</i>)–Fe(18 <i>h</i>)	2.6366(2)	2.6345(2)	2.6329(1)
Fe(12 <i>j</i>)–Fe(6 <i>g</i>)	2.4594(1)	2.4590(1)	2.4596(1)	Fe(18 <i>f</i>)–Fe(9 <i>d</i>)	2.4516(2)	2.4521(3)	2.4538(2)
Fe(12 <i>k</i>)–Fe(12 <i>k</i>)	2.4937(5)	2.4812(5)	2.4825(5)	Fe(18 <i>h</i>)–Fe(18 <i>h</i>)	2.5573(2)	2.5431(5)	2.5503(2)
Fe(12 <i>k</i>)–Fe(6 <i>g</i>)	2.4567(3)	2.4588(3)	2.4611(3)	Fe(18 <i>h</i>)–Fe(9 <i>d</i>)	2.4863(1)	2.4856(3)	2.4858(1)

Fe(12*k*)–Fe(12*k*) interactions are weakly negative. The substitution of nonmagnetic Ga atoms at iron 12*k* site reduces the negative exchange interactions. At the same time, nonmagnetic Ga atoms dilute the magnetic Fe sublattice. This creates a strong competition between the magnetic exchange and magnetic dilution effects but, the magnetic exchange dominates over the reduction of positive exchange interactions, thereby accounting for the increase in Curie temperature.

The results of neutron diffraction study confirm that the increase in Curie temperature in the present study with substitution of Ga at Fe sites and insertion of carbon at the interstitial sites is not a result of increased distance at Fe–Fe dumb-bell site but rather due to expansion of Fe–Fe bonds at 12*j*(18*f*) and 12*k*(18*h*) sites where Ga shows preferential occupancy as shown in Table III. The reduction in negative exchange interactions appears to have the main influence on increase in Curie temperature while further increase in Curie temperature upon carbonation can be attributed to the lengthening of Fe–Fe bonds. The 4*f* sites of Fe which have been assumed to be mainly associated with the magnetic exchange coupling and hence Curie temperature, are completely unoccupied by Ga atoms.

Analysis of the interatomic distances suggests that the carbon atom is strongly bonded to its nearest Fe neighbors. The Fe(18*h*)–C bond lengths are 1.9298, 1.9388, and 1.9476 Å in the compounds Ho₂Fe₁₅Ga₂C₂, Er₂Fe₁₅Ga₂C₂, and HoErFe₁₅Ga₂C₂ respectively, showing the strong covalent character of Fe–C bonds. Such a short ‘‘Fe–*p* element’’ bond length was reported earlier in R₂Fe₁₄B.¹⁹ The 6*c* site has the largest number of nearest Fe neighbors and the largest magnetic moment ($\sim 3\mu_B$) in the rhombohedral Th₂Zn₁₇ type structure as shown in Table I. The lowest magnetic moment ($\sim 1.2\mu_B$) belongs to the Fe atoms (18*h*) directly bonded to the interstitial element. The moments for Ho and Er atoms couple antiferromagnetically to the Fe sublattice, as expected.

The easy direction of magnetization at room temperature can be deduced from the x-ray diffractograms taken on the

magnetically aligned powders where the enhanced (00*l*) or (*hk*0) reflections indicate that the easy magnetization direction is parallel or perpendicular to the crystallographic *c* axis. In Fig. 3, the strong enhancement in the intensities of reflections (300) and (220) together with the absence of other reflections clearly demonstrate that the easy magnetization direction lies in the basal plane at room temperature.

ACKNOWLEDGMENT

The authors are thankful to Dr. M. S. Ramachandra Rao for fruitful discussions.

- ¹J. M. D. Coey and H. Sun, *J. Magn. Magn. Mater.* **87**, L251 (1990).
- ²K. H. J. Buschow, *Rep. Prog. Phys.* **40**, 1179 (1977).
- ³K. S. V. L. Narasimham, W. E. Wallace, and R. D. Hutchers, *IEEE Trans. Magn.* **MAG-10**, 729 (1974).
- ⁴X. C. Kou, R. Grössinger, T. H. Jacobs, and K. H. J. Buschow, *Physica B* **168**, 181 (1991).
- ⁵L. Hu and W. B. Yelon, *J. Appl. Phys.* **76**, 6147 (1994).
- ⁶K. G. Suresh and K. V. S. Rama Rao, *J. Appl. Phys.* **79**, 345 (1996).
- ⁷M. Venkatesan, U. V. Varadaraju, and K. V. S. Rama Rao, *J. Magn. Magn. Mater.* **182**, 231 (1998).
- ⁸M. Merches, W. E. Wallace, and R. S. Craig, *J. Magn. Magn. Mater.* **24**, 97 (1981).
- ⁹H. Fujii and H. Sun, in *Handbook of Magnetic Materials*, edited by K. H. J. Buschow (Elsevier, Netherlands, 1995), Vol. 9, p. 303.
- ¹⁰M. Venkatesan, U. V. Varadaraju, and K. V. S. Rama Rao, *The Third Pacific Rim International Conference on Advanced Materials and Processing (PRICM 3)*, edited by M. A. Imam, 1998, p. 971.
- ¹¹H. M. Rietveld, *J. Appl. Crystallogr.* **2**, 65 (1969).
- ¹²FULLPROF Rietveld refinement code written by J. Rodriguez-Carjaval, Institute Laue Langevin, Grenoble, France.
- ¹³G. Block and W. Jeitschko, *Inorg. Chem.* **25**, 279 (1968).
- ¹⁴G. Block and W. Jeitschko, *J. Solid State Chem.* **70**, 271 (1987).
- ¹⁵R. B. Helmholtz and K. H. J. Buschow, *J. Less-Common Met.* **155**, 15 (1985).
- ¹⁶C. Lin, Y. X. Liu, H. W. Jiang, J. L. Yang, B. S. Zhang, and Y. F. Deng, *Solid State Commun.* **81**, 299 (1992).
- ¹⁷G. J. Long, G. K. Marasinghe, S. Mishra, O. A. Pringle, F. Grandjean, K. H. J. Buschow, D. P. Middleton, W. B. Yelon, F. Pourarian, and O. Isnard, *Solid State Commun.* **88**, 761 (1993).
- ¹⁸D. Givord and R. Lemaire, *IEEE Trans. Magn.* **MAG-10**, 109 (1974).
- ¹⁹D. Fruchart, S. Miraglia, S. Obbade, R. Verhoef, and P. Wolfers, *Physica B* **180-181**, 578 (1992).